Celal Bayar University Journal of Science

High Isolation Wideband Multiple-Input Multiple-Output Antennas for Millimeter Wave Applications

Tayfun Okan[1]*

[1] Electrical and Electronics Engineering, University of Turkish Aeronautical Association, Ankara, Turkey
*tokan@thk.edu.tr
*Orcid: 0000-0002-9913-0803

Received: 12 May 2020
Accepted: 5 December 2020
DOI: 10.18466/cbayarfbe.736444

Abstract

A planar 2×2 and 4×4 multiple-input multiple-output (MIMO) antennas are designed and analyzed in this study. The individual antenna elements that form the MIMO structure are located perpendicular to each other in order to facilitate polarization diversity. Except a notch band at 4.3 GHz, the 2×2 antenna nearly covers the entire 2.41-31.4 GHz frequency band. It is similar for the 4×4 antenna that has tri-band characteristic, where the impedance bandwidth ($|S_{11}| \leq -10$ dB) values are determined as 1.4, 10.05 and 16.26 GHz. Beside these high bandwidth results, both MIMO antennas have perfect isolation characteristic which is important to prevent coupling in MIMO systems. The proposed MIMO antennas are convenient to be used in all *S* (2-4 GHz), *C* (4-8 GHz), *X* (8-12 GHz), *Ku* (12-18 GHz) and *K*-bands (18-27 GHz). Furthermore, omnidirectional radiation patterns are observed at the resonance frequencies, and the reported 2×2 and 4×4 antennas have compact sizes of 80×40×1 mm^3 (64.5λ×32.25λ ×0.8λ) and 80×80×1 mm^3 (64.5λ×64.5λ ×0.8λ), respectively.

Keywords: Millimeter wave, monopole antenna, multiple-input multiple-output (MIMO).

1. Introduction

With the continuously developing technology, there is a high demand to monopole antennas because of their ease of fabrication, small size and wide bandwidth. Therefore, monopole antennas are used frequently in a variety of millimeter wave applications. For instance, they are used inside human body as a biocompatible implanted antenna operating at industrial, scientific and medical (ISM) band [1, 2]. They are also used with many wireless communication systems like 5G technology [3, 4], wireless local area network (WLAN) [5], wireless fidelity (wi-fi) applications [6, 7], vehicular applications [8], satellite communication systems and even with wearable antennas [9, 10]. Furthermore; when the need to a wide impedance bandwidth arises, monopole antennas are still considered to be implemented in ultra-wideband (UWB) [11, 12] and super wideband (SWB) [13] antenna designs. In [14], a nona-band loop monopole antenna is reported to be used for mobile handset. The bandwidth and directivity of a monopole antenna is enhanced with the help of a magnetic metamaterial slab used over the ground plane in [15]; whereas, the directivity is improved with a left-handed medium metamaterial unit cell in [16]. Another monopole antenna is presented in [17], where signal interference technique and circular disk designed antenna are employed to form a filtering antenna structure.

Multiple-input multiple-output (MIMO) antennas have many advantages like offering a high data rate and high quality of service (QoS), reducing bit error rate (BER) and supporting large number of subscribers. Therefore, combining MIMO technology with UWB or SWB antenna designs ensure a further improvement in the quality and performance [18]. A wideband MIMO antenna is designed in [4] to be used for the future mobile devices operating in the 5G technology. MIMO antennas are used for base station applications as well [19], where the presented tri-band multi polarized MIMO antenna is reported to have a resonance at 28/38/48 GHz frequencies. It is important to note that in most of the former MIMO antenna studies, the MIMO design is generally created by positioning the individual antennas perpendicular to each other to facilitate polarization diversity. In [20], MIMO antennas are compared with directional slot and conventional slot antenna designs. The MIMO antennas proposed in [21, 22] operate at around 3.5 GHz and 5.5 GHz wireless communication systems, respectively. A 2×2 MIMO antenna is developed in [23] with coplanar waveguide

Celal Bayar University Journal of Science
Volume 16, Issue 4, 2020, p 355-360
Doi: 10.18466/cbayarfbe.736444

technique, where the antenna is designed to operate at both 3.5 and 5.5 GHz frequencies. As seen from the abovementioned studies, MIMO antennas are frequently employed for wireless communication systems [24, 25] thanks to their high data rate feature.

In our previous study [13], a SWB antenna that operates between 2.59 to 31.14 GHz frequency band with a reflection coefficient of $|S_{11}| \leq -10$ dB was designed. The reported antenna had a bandwidth of 28.55 GHz and fractal bandwidth of 169%. Moreover, it had a compact size with the dimensions of 40×40×1 mm^3. The single element radiation characteristics were proposed by analyzing the parameters like return loss, realized gain, radiation efficiency, far-field radiation pattern and surface current distribution. Successful results were obtained when compared with other state-of-arts for the designed SWB antenna.

Using MIMO technology with wideband monopole antennas yields further enhancements in the speed of data transfer. Hence, the reported SWB antenna in our previous study is combined with MIMO technology in this study. A 2×2 and a 4×4 MIMO versions of the design are tested with CST Microwave Studio, a computer-based simulation program; where the reflection coefficient, isolation, diversity gain (DG) and envelope correlation coefficient (ECC) parameters of the proposed MIMO antennas are analyzed. It is observed that in the frequency range from 2.41 GHz to 31.4 GHz, the 2×2 and 4×4 MIMO antennas have dual-band and tri-band characteristics, respectively. Besides that, the wide bandwidth feature of the antenna is well maintained and both of the proposed MIMO antenna designs exhibit high isolation performance. Another importance of this study is that, an improvement is achieved in data rate and QoS, thanks to multipath property of the MIMO structure.

2. Antenna Design

A 2×2 and 4×4 MIMO antennas are analyzed in this study that consist of 2 layers as seen in Fig. 1. An octagonal shaped radiator is used for wide bandwidth. The radiator and microstrip transmission line are shifted to the left from the center part, in order to increase the impedance bandwidth. The width and length of the feeding line is determined to match the 50 Ω characteristic impedance. A stub is inserted to the right top of the radiator, and a small sized notch is introduced to the ground plane to further improve the bandwidth. The location of the notch is determined as to be on the projection of the transmission line. Rogers RT5880 substrate with a loss tangent of 0.0009 and a permittivity of 2.2 is used with a thickness of 1 mm. The bright and dark parts seen in Fig. 1, represents the substrate and copper parts of the antenna, respectively. MIMO designs are formed by positioning the antenna elements orthogonal to each other. Moreover, copper thickness is used as 0.035 mm and the parameters of the proposed antenna is given in Table 1. The overall dimensions of the proposed 2×2 and 4×4 MIMO antenna designs are 80×40×1 mm^3 (64.5λ×32.25λ ×0.8λ) and 80×80×1 mm^3 (64.5λ×64.5λ ×0.8λ) respectively, where λ is the wavelength for the smallest operating frequency. Therefore, W_1, W_2 and L_1 are 80 mm, L_1 has a value of 40 mm.

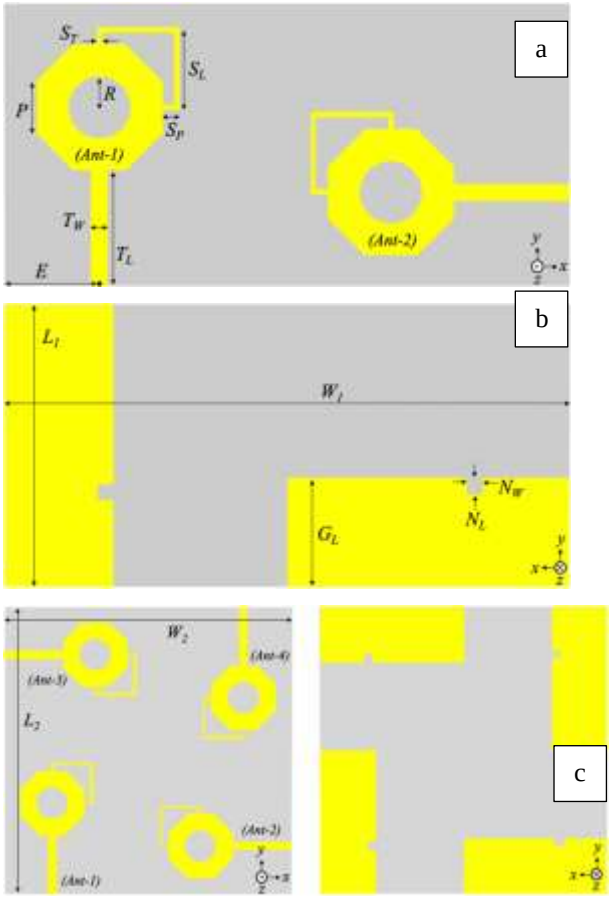

Figure 1. The geometry of the proposed MIMO antenna (a) top view of the 2×2 version (b) bottom view of the 2×2 version (c) top and bottom view of the 4×4 version.

Table 1. Parameters of the proposed MIMO antennas.

Parameters	S_L	S_T	S_P	P
Value (mm)	11.65	0.65	2.38	7.35
Parameters	G_L	N_L	N_W	T_L
Value (mm)	15.42	2.34	2.27	16.41
Parameters	T_W	R	E	
Value (mm)	2.37	4.43	13.34	

3. Results and Discussion

The performance of 2×2 and 4×4 antenna structures are analyzed and interpreted under this title by using the results obtained from CST Microwave Studio. S-parameters versus frequency graph of the 2×2 antenna is

Celal Bayar University Journal of Science
Volume 16, Issue 4, 2020, p 355-360
Doi: 10.18466/cbayarfbe.736444

depicted in Fig.2(a), whereas the VSWR graph is plotted in Fig.2(b). As seen from Fig.2(a), the simulated return loss results of both of the antenna elements (S_{11}, S_{22}) in 2×2 design align well with each other. As the return loss curves rise above the -10 dB at 4.3 GHz, the antenna elements have dual band between 2.41-31.4 GHz interval. The impedance bandwidth ($|S_{11}| \leq -10$ dB) of 2×2 antenna is 1.69 GHz (2.41-4.1 GHz) and 26.85 GHz (4.55-31.4 GHz), respectively. It is also possible to say that the 2×2 MIMO antenna has an operating bandwidth from 2.41 GHz to 31.4 GHz excluding 4.3 GHz notch band. When the insertion loss (S_{12}, S_{21}) analysis is performed, it is seen that the values are kept below -25 dB through the operating frequency range. This means that, the isolation between the antenna elements are successfully provided. The success in providing a good impedance matching for the designed antenna is also measured by analyzing VSWR values; since VSWR is dependent on the reflection coefficient (Γ) with the formula of $VSWR = \frac{1+|\Gamma|}{1-|\Gamma|}$. As seen from Fig. 2(b), VSWR values are kept below 2 in the entire simulated frequency range.

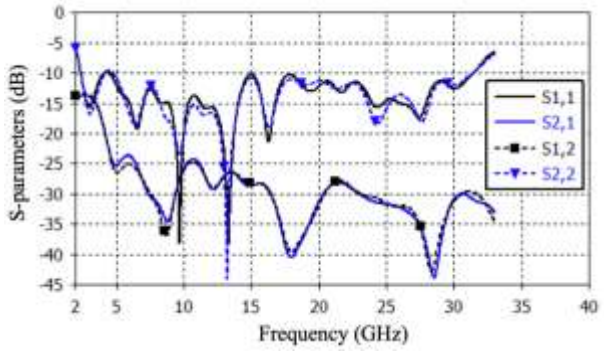

(a)

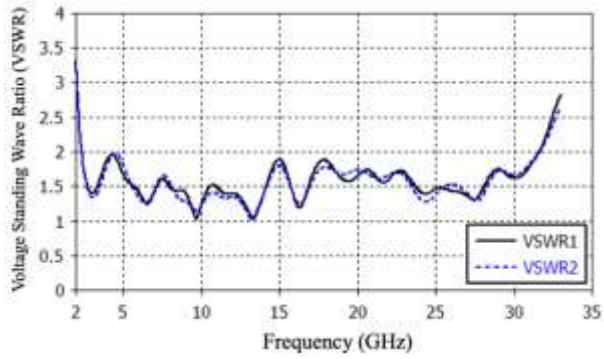

(b)

Figure 2. (a) The return loss and insertion loss graph, (b) VSWR graph of 2×2 MIMO antenna.

Same analyses are made for the 4×4 design, as seen from Fig. 3. The four return loss and VSWR curves of each antenna element are overlapping, which proves that each element performs the same characteristic. This design has three separate bands in the operating frequency range, the bandwidths of which are determined as 1.4 GHz (2.41-3.81 GHz), 10.05 GHz (4.78-14.83 GHz) and 16.26 GHz (15.24-31.5 GHz), respectively. Furthermore, the insertion loss values are almost always below -20 dB. As this design has multiple bands, the VSWR value at 4.3 GHz rises above 2 as seen in Fig. 3(b). The bandwidth values of 2×2 and 4×4 antennas are given in Table 2, where they are compared with our previous single element antenna design [13]. One can say that, as the number of antenna elements increases in the MIMO structure, the bandwidth of the antennas decreases and the number of bands appearing in the operating range increases. On the other hand, the isolation between the antenna elements are well maintained in both 2×2 and 4×4 MIMO antenna designs.

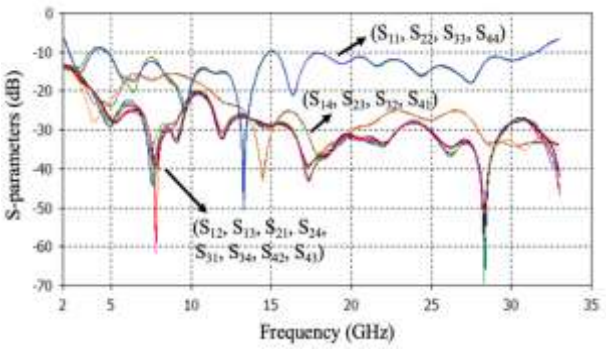

(a)

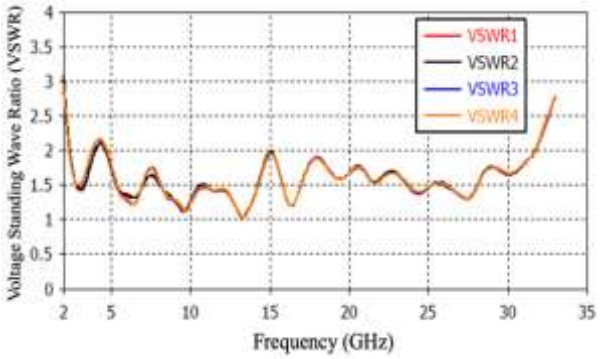

(b)

Figure 3. (a) The return loss and insertion loss graph, (b) VSWR graph of 4×4 MIMO antenna.

Table 2. Parameters of the proposed MIMO antennas.

Design	BW-1	BW-2	BW-3
Single antenna element [13]	28.55 GHz (2.59-31.14 GHz)	-	-
2×2	1.69 GHz (2.41-4.1 GHz)	26.85 GHz (4.55-31.4 GHz)	-
4×4	1.4 GHz (2.41-3.81 GHz)	10.05 GHz (4.78-14.83 GHz)	16.26 GHz (15.24-31.5 GHz)

* BW-i: i*th* bandwidth.

The vectoral surface current distribution of the MIMO antennas are shown in Fig. 4. As seen from the figure, Ant-1 is the excited element for both 2×2 and 4×4 structures. The simulations are performed at 13.3 GHz, since both structures have a resonance frequency at 13.3 GHz. The surface currents are concentrated mainly at the edge of the feeding line and they also seem to be denser at the stub located on the top right corner of the radiator patch. Both 2×2 and 4×4 structures are nearly in the same current distribution form, as they are both measured at 13.3 GHz.

Radiation pattern is another important antenna property that defines the radiation behavior of the antenna [26]. The far field radiation patterns of 2×2 and 4×4 structures are depicted in polar form in Fig. 5. The simulations for *E* (xz-plane) and *H* (yz-plane) planes are performed at 13.3 GHz resonance frequency and it is observed that both MIMO antennas have omni-directional radiation characteristic.

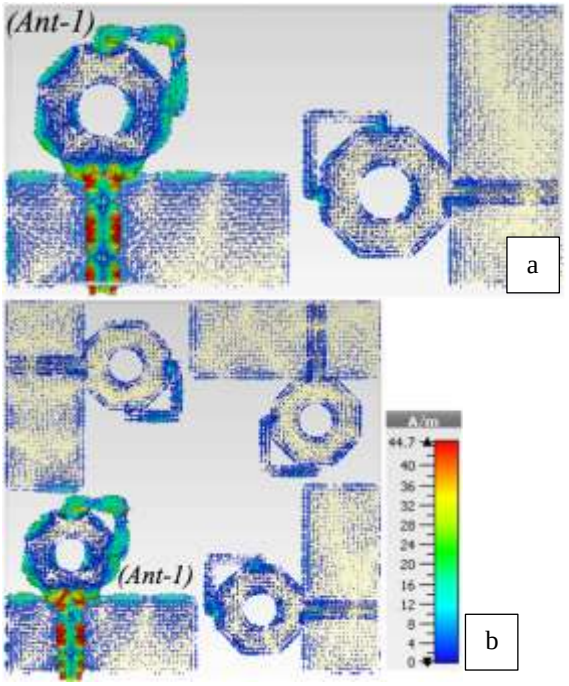

Figure 4. Vectoral surface current distribution of the proposed (a) 2×2 and (b) 4×4 MIMO antennas at 13.3 GHz, when Ant-1 is excited.

Diversity gain (DG) and envelope correlation coefficient (ECC) are other parameters that need to be examined to analyze the performance of MIMO antennas. The numerical expressions of ECC and CG are given in Eq. (3.1) and (3.2), respectively. As seen from Eq. (3.1), the ECC value at a certain frequency is dependent on the return loss and insertion loss values at that frequency. The ideal value of ECC is expected to be 0.1 or less and it is expected to be higher than 9.5 for DG. As seen from Fig. 6(a), both MIMO antennas have an ECC value below 0.01; and even between 4.5 GHz to 31 GHz it is below 0.001, which is a very successful result. This shows that the antennas that form the MIMO structure are independent of each other. It is important to emphasize that positioning the antenna elements perpendicular to each other has an effect on this low ECC value. Same successful results are obtained for DG as seen in Fig. 6(b), which is higher than 9.995 in the operating frequency range.

$$ECC = \frac{|S_{11}^{*}S_{12}+S_{21}^{*}S_{22}|^2}{(1-(|S_{11}|^2+|S_{21}|^2))(1-(|S_{22}|^2+|S_{12}|^2))} \quad \textbf{(3.1)}$$

$$DG = \sqrt{100-100ECC)} \quad \textbf{(3.2)}$$

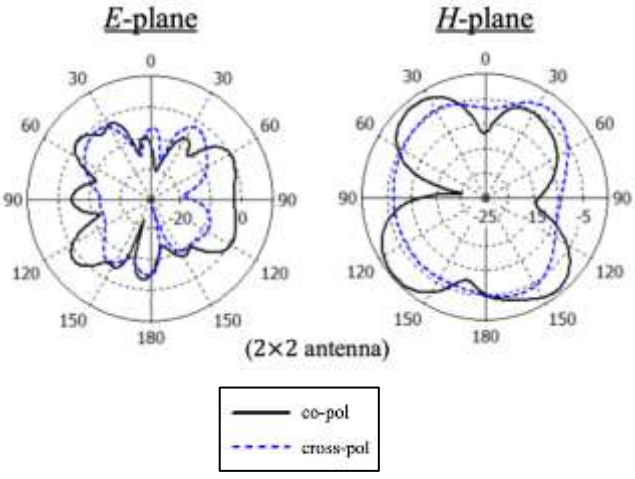

Celal Bayar University Journal of Science
Volume 16, Issue 4, 2020, p 355-360
Doi: 10.18466/cbayarfbe.736444

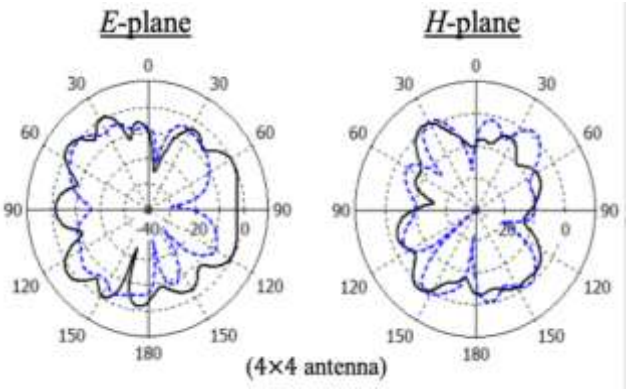

Figure 5. Far field radiation patterns of Ant-1 at 13.3 GHz for the MIMO antennas.

In Table 3, the proposed MIMO antennas are compared with other MIMO antennas that are most recently reported in literature. As seen from the comparison table, both of the presented MIMO antennas have the highest impedance bandwidth of all. Apart from the one reported in [27], the proposed antennas in this study have better isolation and ECC value. On the other hand, except the antenna in [28], the proposed 2×2 and 4×4 MIMO designs have larger sizes than the antennas reported in [27, 29, 30].

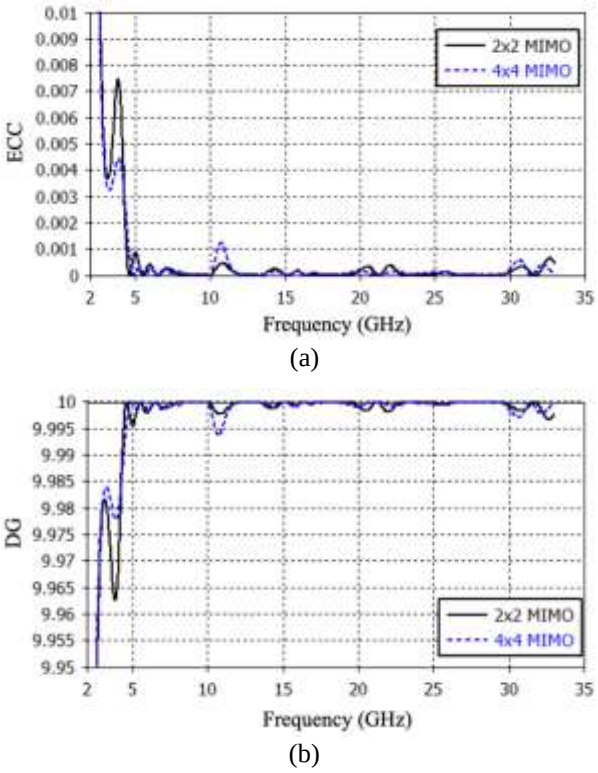

Figure 6. The simulated (a) envelope correction coefficient and (b) diversity gain results of the proposed 2×2 and 4×4 antennas.

Table 3. Comparison with other studies available on literature.

Reference	Structure	Size (mm^2)	No. of Bands	Operating Bands (GHz)	Bandwidth	Isolation (dB)	ECC
[29]	4×4	45×45	3	3-5 6-8.5 9.3-10.6	2 2.5 1.3	<-17	<0.08
[30]	4×4	40×40	1	3-11	8	<-15	<0.006
[27]	2×2	50×30	1	2.5-15	12.5	<-20	0.04
[28]	-	60×60	1	2.35-2.45	0.1	<-18	<0.002
Proposed	2×2	80×40	2	2.41-4.1 4.55-31.4	1.69 26.85	<-25	<0.0005
Proposed	4×4	80×80	3	2.41-3.81 4.78-14.83 15.24-31.5	1.4 10.05 16.26	<-20	<0.0005

4. Conclusion

The 2×2 and 4×4 versions of the previously reported planar SWB monopole antenna are developed and analyzed in this study. MIMO antenna structures are formed by positioning the single antenna elements perpendicular, which facilitates polarization diversity. The 2×2 antenna has an impedance bandwidth ($|S_{11}| \leq -10$ dB) of 1.69 and 26.85 GHz; whereas the 4×4 antenna's bandwidth values are calculated as 1.4, 10.05 and 16.26 GHz. Therefore, the presented MIMO antennas are suitable to be used with millimeter wave applications. Successful results are obtained from the simulated insertion loss and ECC values. The 2×2 and 4×4 antennas have dimensions of 80×40×1 and 80×80×1 mm^3 respectively, so they can be implemented easily in portable devices. Owing to all these aforementioned features the proposed MIMO antennas are appropriate to be used in many different applications operating at many different frequency bands.

Author's Contributions

Tayfun Okan: Drafted and wrote the manuscript, performed the experiment and result analysis.

Ethics

There are no ethical issues after the publication of this manuscript.

References

1. Isaac, AA, Al-Rizzo, H, Yahya, S, Al-Wahhamy, A, Tariq, SZ. 2020. Miniaturized MIMO antenna array of two vertical monopoles embedded inside a planar decoupling network for the 2.4 GHz ISM band. *IET Microwaves, Antennas & Propagation;* 14(1): 132-140.

2. Li, PK, You, CJ, Yu, HF, Cheng, YJ, Yang, YW, Deng, JH. 2018. A high frequency ratio quadri-band frequency independently tunable antenna with spurious-mode suppression. *Microwave and Optical Technology Letters*; 60: 1445–1452.

3. Okan, T. 2020. Design and analysis of a quad-band substrate-integrated- waveguide cavity backed slot antenna for 5G applications. *International Journal of RF and Microwave Computer Aided Engineering*; 30(7): e22236.

4. Cui, L, Guo, J, Liu, Y, Sim, C. 2019. An 8-Element Dual-Band MIMO Antenna with Decoupling Stub for 5G Smartphone Applications. *IEEE Antennas and Wireless Propagation Letters*; 18(10): 2095-2099.

5. Hatami, N, Nourinia, J, Ghobadi, C, Majidzadeh, M, Azarm, B. 2019. High Inter-Element Isolation and WLAN Filtering Mechanism: A Compact MIMO Antenna Scheme. *AEU - International Journal of Electronics and Communications;* 109: 43-54.

6. Mondal, K, Sarkar, PP. 2017. Dual band compact monopole antenna for ISM 2.4/5.8 frequency bands with bluetooth, Wi-Fi, and mobile applications. *Microwave and Optical Technology Letters;* 59(5): 1061–1065.

7. Pazin, L, Kogan, I, Leviatan, Y. 2008. Flat-plate triangular monopole antenna for Wi-Fi/WiMAX/DVB-H applications. *Microwave and Optical Technology Letters*; 50(11): 2922-2925.

8. Werner, PL, Werner, DH. 2005. Design synthesis of miniature multiband monopole antennas with application to ground-based and vehicular communication systems. *IEEE Antennas and Wireless Propagation Letters*; 4: 104-106.

9. Tetik, E, Tetik, GD. 2018. The effect of a metamaterial based wearable monopole antenna on the human body. *Celal Bayar University Journal of Science*; 14(1): 97-93.

10. Gupta, A, Kansal, A, Chawla, P. 2019. Design of a patch antenna with square ring-shaped-coupled ground for on-/off body communication. *International Journal of Electronics*; 106(12): 1814-1828.

11. Toktaş, A, Yerlikaya, M, Yiğit, E. 2016. Microstrip-fed Triangular UWB Microstrip Antenna Based on DGS. *International Journal of Applied Mathematics Electronics and Computers*; (Special Issue-1): 43-47.

12. Biçer, M, Akdağlı, A. 2017. Designing a compact monopole microstrip antenna operating at ultra-wide band for microwave imaging applications. *Turkish Journal of Engineering*; 1(2): 69-66.

13. Okan, T. 2020. A compact octagonal-ring monopole antenna for super wideband applications. *Microwave and Optical Technology Letters;* 62(3): 1237-1244.

14. Liu, Y, Liu, P, Meng, Z, Wang, L, Li, Y. 2018. A Planar Printed Nona-Band Loop-Monopole Reconfigurable Antenna for Mobile Handsets. *IEEE Antennas and Wireless Propagation Letters*; 17(8): 1575-1579.

15. Das, GK, Shaw, T, Mitra, D, Mitra, M. 2019. Directivity enhancement of wire monopole antenna using magnetic metamaterials. *International Journal of RF and Microwave Computer-Aided Engineering*; 29(8): e21778.

16. Tütüncü, B, Urul, B. 2019. LHM Superstrate for High Directivity Microstrip Antenna. *Celal Bayar Üniversitesi Fen Bilimleri Dergisi*; 15(1): 71-74.

17. Li, D, Chen, Z, Liu, Y, Wang, J, Wu, H. 2020. Signal interference-based selectivity-enhancement technique for omnidirectional monopole antenna. *Microwave and Optical Technology Letters*; 62(10): 3203-3208.

18. Kuzu, S, Akçam, N. 2017. Array antenna using defected ground structure shaped with fractal form generated by Apollonius circle. *IEEE Antennas and Wireless Propagation Letters;* 16: 1020-1023.

19. Mahmoud, KR, Montaser, AM. 2018. Performance of tri-band multi-polarized array antenna for 5G mobile base station adopting polarization and directivity control. *IEEE Access*; 6: 8682-8694.

20. Bactavatchalame, P, Rajakani, K. 2020. Compact broadband slot-based MIMO antenna array for vehicular environment. *Microwave and Optical Technology Letters*; 62(5): 2024-2032.

21. Ren, Z, Zhao, A, Wu, S. 2019. MIMO Antenna with Compact Decoupled Antenna Pairs for 5G Mobile Terminals. *IEEE Antennas and Wireless Propagation Letters*; 18(7): 1367-1371.

22. Cheng, Y, Liu, H, Sheng, BQ, Zhu, L. 2020. A compact 4-element MIMO antenna for terminal devices. *Microwave and Optical Technology Letters*; 62(9): 2930-2937.

23. Taghizadeh, H, Ghobadi, CH, Azarm, B, Majidzadeh, M. 2019. Grounded Coplanar Waveguide-fed Compact MIMO Antenna for Wireless Portable Applications. *Radioengineering*; 28(3): 528-534.

24. Cihangir, A, Ferrero, F, Jacquemod, G, Brachat, P, Luxey, C. 2014. Neutralized Coupling Elements for MIMO Operation in 4G Mobile Terminals. *IEEE Antennas and Wireless Propagation Letters*; 13: 141-144.

25. Aslan, B, Dikmen, O, Kulac, S, Elbir, AM. 2018. Evaluation of Reconfigurable Multiple and Compact Micro-Strip Antennas for MIMO Systems. *Balkan Journal of Electrical and Computer Engineering*; 6: 46-50.

26. Okan, T, Akçam N. 2018. Analysis of antennas around NURBS surfaces by using a hybrid method. *Radioengineering;* 27(3): 703-710.

27. Tripathi, S, Mohan, A, Yadav, S. 2015. A compact koch fractal UWB MIMO antenna with WLAN band-rejection. *IEEE Antennas and Wireless Propagation Letters*; 14 (4): 1565–1568.

28. Ali, WAE, Ibrahim, AA. 2017. A compact double-sided MIMO antenna with an improved isolation for UWB applications. *AEU - International Journal of Electronics and Communications*; 82: 7–13.

29. Iqbal, A, Saraereh, OA, Ahmad, AW, Bashir, S. 2018. Mutual coupling reduction using F- shaped stubs in UWB MIMO antenna. *IEEE Access*; 6: 2755–2759.

30. Yu, K, Li, Y, Liu, X. 2018. Mutual coupling reduction of a MIMO antenna array using 3-D novel meta-material structures. *ACES Journal;* 33(7): 758-763.